Available online at www.sciencedirect.com
ScienceDirect
Advances in Water Resources 29 (2006) 1479–1489
Advances in Water Resources
www.elsevier.com/locate/advwatres

A novel analytical solution for a slug test conducted in a well with a finite-thickness skin

Hund-Der Yeh [a,*], Shaw-Yang Yang [b]

[a] Institute of Environmental Engineering, National Chiao Tung University, 75, Po-Ai Street, Hsinchu 30039, Taiwan
[b] Department of Civil Engineering, Vanung University, Chungli, Taiwan

Received 17 August 2005; accepted 2 November 2005
Available online 5 January 2006

Abstract

An aquifer containing a skin zone is considered as a two-zone system. A mathematical model describing the head distribution is presented for a slug test performed in a two-zone confined aquifer system. A closed-form solution for the model is derived by Laplace transforms and Bromwich integral. This new solution is used to investigate the effects of skin type, skin thickness, and the contrast of skin transmissivity to formation transmissivity on the distributions of dimensionless hydraulic head. The results indicate that the effect of skin type is marked if the slug-test data is obtained from a radial two-zone aquifer system. The dimensionless well water level increases with the dimensionless positive skin thickness and decreases as the dimensionless negative skin thickness increases. In addition, the distribution of dimensionless well water level due to the slug test depends on the hydraulic properties of both the wellbore skin and formation zones.

Keywords: Ground water; Slug test; Confined aquifer; Skin effect; Laplace transforms; Closed-form solution

1. Introduction

A slug test is one of the aquifer test methods commonly used to investigate aquifer parameters. The test involves an instantaneous removal/injection of a small volume of water from/into a well [7]. An instantaneous head change is thus imposed within a well and the recovery/falloff of water level is continuously measured using a pressure transducer that connects to a data logger. The aquifer parameters, e.g., transmissivity and storativity, can then be obtained if the slug-test data is analyzed.

Ferris and Knowles [12] originally introduced the analysis procedure from slug-test data. They derived an approximate solution for describing the water level change within the test well. The transmissivity is estimated based on a straight line, which represents residual head versus inverse time. Employing an electrical analog model of the well-aquifer system, Bredehoeft et al. [4] demonstrated that Ferris and Knowles' approximation is valid only for very late test time. Using the modified Thiem equation for the unconfined and steady state conditions, Bouwer and Rice [3] presented a procedure for determining the hydraulic conductivity or transmissivity for the unconfined aquifers. Using results from an electric analog model, they obtained two empirical formulas related to the effective radius for the partially and fully penetrating wells. Later, Bouwer [2] provided information on using Bouwer and Rice's method for testing the validity of falling level tests, the application of the method to the confined aquifers, the effect of well diameter, and the computer processing of field data. Cooper et al. [8] obtained a solution including the well storage analogous to a heat conduction problem provided by Carslaw and Jaeger [6]. Cooper et al. [8] applied their solution to a ground-water flow system and made a

* Corresponding author. Fax: +886 3 5726050.
E-mail address: hdyeh@mail.nctu.edu.tw (H.-D. Yeh).

0309-1708/$ - see front matter © 2005 Published by Elsevier Ltd.
doi:10.1016/j.advwatres.2005.11.002

Nomenclature

T	Transmissivity
S	Storativity
r	Radial distance from the centerline of the well
r_w	Radius of the well
r_c	Radius of the standpipe
r_s	Radial distance from the well centerline to the outer skin envelope
t	Time from the start of the test
H	Hydraulic head distribution
H_0	Initial hydraulic head in the wellbore skin and formation zones
$\overline{H}$	Hydraulic head in the Laplace domain
q^2	pS/T
p	Laplace variable
$J_0(\cdot)$, $Y_0(\cdot)$	Bessel functions of the first and second kinds of order zero
$J_1(\cdot)$, $Y_1(\cdot)$	Bessel functions of the first and second kinds of order one
$I_0(\cdot)$, $K_0(\cdot)$	Modified Bessel functions of the first and second kinds of order zero
$I_1(\cdot)$, $K_1(\cdot)$	Modified Bessel functions of the first and second kinds of order one
κ	$\sqrt{T_1 S_2/T_2 S_1}$
ζ	T_2/T_1
η	S_2/S_1
α	$S_2 r_w^2/r_c^2$
β	$T_2 t/r_c^2$
ρ	r/r_w
ρ_c	r_c/r_w
ρ_s	r_s/r_w
$\bar{h}$	$\overline{H}/H_0$
h	H/H_0
λ_1^2	$\zeta p/\eta$
λ_2^2	p

Subscripts

1, 2	Wellbore skin, formation

family of type curves. They used a matching approach for the slug-test data to estimate aquifer parameters. However, the aquifer parameters obtained by this technique may be very rough because the shape of a type curve is rather insensitive to the value of aquifer storage [19], especially, if the storage is very small. Kipp [17] constructed a set of type curves that enables the well water level response data from the slug tests to be analyzed if the inertial parameter is large. Pandit and Miner [23] provided an automatic fitting procedure to determine the aquifer parameters when analyzing the slug-test data obtained from a confined aquifer. Marschall and Barczewski [20] presented an analysis of slug tests in the frequency domain for evaluating the solution of Cooper et al. [8]. Their solution is in terms of Kelvin functions [18], and the slug-test data is transformed using numerical Fourier transforms to determine aquifer parameters. Such an approach can avoid evaluating the integrand, which is an oscillatory function and difficult to evaluate.

Using the infinitesimally thin skin concept, Ramey and Agarwal [24] reported a solution to the drill-stem test (DST) problem with an inversion integral and related short- and long-time approximating forms. The skin effect describing the damage or improvement to the region surrounding a well is represented by a skin factor. Ramey et al. [25] presented semi- and double-log type curves, which combine the effects of the well storage and wellbore skin, to determine the formation permeability and skin effect by analyzing the slug-test data. Faust and Mercer [11] provided an infinite-aquifer solution for the response of slug tests to investigate the effect of a finite-thickness skin. They assumed that the skin has a much lower permeability than that of the adjacent formation. Under this condition, the skin effect can lead to very low estimates of hydraulic conductivity if using the type-curve fitting method of Cooper et al. [8]. Moench and Hsieh [21] commented on the evaluation of slug tests in a finite-thickness skin by Faust and Mercer [11]. They showed that when the specific storage of the skin is negligibly small, the finite-thickness skin solution becomes equivalent to the infinitesimally thin skin solution. Under a finite-thickness skin condition, the skin properties control the early time response, whereas the formation properties relate to the late time response. Further, Sageev [26] investigated the effects of the well storage and wellbore skin in a confined aquifer system. He obtained a similar result to that of Moench and Hsieh [21]. Karasaki et al. [16] developed various slug-tests models and related solutions for linear flow, radial flow with boundaries, two zone, and concentric composite aquifer systems. They provided type curves for each solution and noted that slug tests suffer the problem of non-uniqueness in matching the test data to type curves. Butler and Healey [5] investigated the estimate of hydraulic conductivity obtained through the pumping or slug test. They indicated that the hydraulic conductivity estimate from a pumping test is, on the average, larger than that from a series of slug test in the same formation.

An aquifer is considered as a radial two-zone (or composite) system if the formation properties near the well is apparently changed due to the well drilling or development. Well drilling causes the invasion of drilling

mud into the aquifer and may produce a positive wellbore skin that has lower permeability than that of the original formation. On the other hand, the extensive well development and/or substantial spalling and fracturing of the borehole wall may increase the permeability of the formation around a well. Under such circumstances, the disturbed formation is referred to as a negative wellbore skin. Moench and Hsieh [22] presented a Laplace-domain solution for the well response to a drill-stem test in the presence of skin. They found that the standard methods of analysis are adequate for open-well slug tests and may differ markedly in the pressure response for pressurized slug tests. Karasaki [15] used the time convolution method of Duhamel's theorem to evaluate the solution of Moench and Hsieh [22]. The systematized procedure and analysis method were proposed for a drill-stem test. Recently, Yang and Gates [31] constructed a finite-element model for a slug test in a confined aquifer system considering the effect of a finite-thickness skin. They suggested that the effect of a wellbore skin on the estimate of hydraulic conductivity for low-permeability mediums could be minimized by the use of the late-time data.

A mathematical model describing the head distributions in the skin and formation zones is presented for a slug test performed in a two-zone confined aquifer. The objective of this paper is to derive a new analytical solution in terms of hydraulic head for slug tests conducted in such a radial two-zone system. The solution is solved by applying Laplace transforms to the governing equations and related boundary conditions of the model and the Bromwich integral [13] to the Laplace-domain solution. The solution in the time domain is expressed in terms of an integral that covers a range from zero to infinity and has an integrand consisting of complicate products terms of Bessel functions. This newly derived solution is evaluated by numerical approaches and compared with that of Cooper et al.'s solution [8] for a uniform media and the results of numerical inversion from the Laplace-domain solution. The solution is employed to investigate the effects of skin type, skin thickness, and the contrast of skin transmissivity to formation transmissivity on the distributions of dimensionless hydraulic head.

2. Mathematical derivations

2.1. Mathematical statement

Fig. 1 displays the well and aquifer configurations for a radial two-zone confined aquifer system. The assumptions made for this aquifer system are: (1) the aquifer is homogeneous, isotropic, infinite-extent, and with a constant thickness, (2) the well is fully penetrating and with a finite radius, (3) the initial head is constant and uniform throughout the whole aquifer, and (4) the vertical flow gradients are negligible. Under these assumptions, the governing equations for the head distributions in the skin and formation zones can respectively be written as

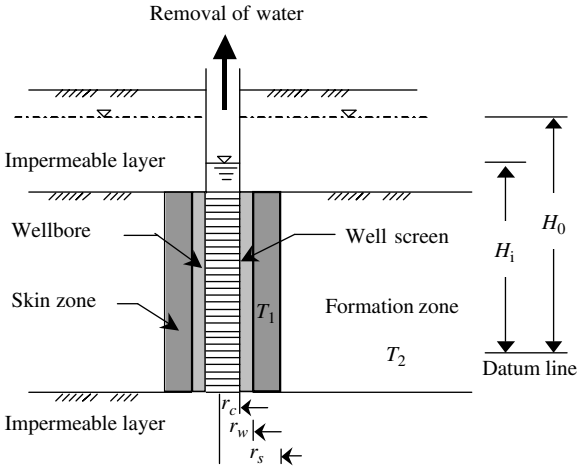

Fig. 1. Schematic diagram of the well and aquifer configurations.

$$\frac{\partial^2 H_1}{\partial r^2}+\frac{1}{r}\frac{\partial H_1}{\partial r}=\frac{S_1}{T_1}\frac{\partial H_1}{\partial t}, \quad r_w \leqslant r \leqslant r_s \tag{1}$$

and

$$\frac{\partial^2 H_2}{\partial r^2}+\frac{1}{r}\frac{\partial H_2}{\partial r}=\frac{S_2}{T_2}\frac{\partial H_2}{\partial t}, \quad r_s \leqslant r < \infty \tag{2}$$

where the subscripts 1 and 2, respectively, denote the skin and formation zones; H (or $H(r, t)$) is hydraulic head; r is radial distance from the well centerline; r_w is well radius; r_s is radial distance from the well centerline to the outer skin envelope; t is time from the start of test; S is storativity; and T is transmissivity.

The hydraulic heads are initially assumed to be zero in both the skin and formation zones, that is

$$H_1(r,0)=H_2(r,0)=0, \quad r > r_w \tag{3}$$

The initial condition for hydraulic head in a well is

$$H_1(r_w,0)=H_0 \tag{4}$$

where H_0 is the initial hydraulic head in aquifer. When $r=r_w$, the hydraulic head represents the well water level if the well loss is negligible. The hydraulic head in the formation tends to zero as r approaches infinity, that is

$$H_2(\infty,t)=0 \tag{5}$$

The conservation of mass at a well requires that

$$\pi r_c^2\left(\frac{\partial H_1}{\partial t}\right)_{r=r_w}=2\pi r_w T_1\left(\frac{\partial H_1}{\partial r}\right)_{r=r_w} \tag{6}$$

where r_c is the standpipe radius. The hydraulic head is continuous at the interface between the skin and formation zones, i.e.,

$$H_1(r_s,t) = H_2(r_s,t), \quad t>0 \tag{7}$$

and the continuity of flow rate between the skin and formation zones requires

$$T_1\frac{\partial H_1(r_s,t)}{\partial r} = T_2\frac{\partial H_2(r_s,t)}{\partial r}, \quad t>0 \tag{8}$$

2.2. Closed-form solutions

The Laplace-domain solution for the hydraulic heads in both the skin and formation zones can be obtained by taking Laplace transforms of Eqs. (1)–(8). The results for $\overline{H}_1$ and $\overline{H}_2$ are respectively expressed as

$$\overline{H}_1 = \frac{r_w S_2 H_0}{T_1 q_1}\left[\frac{-\Phi_1 I_0(q_1 r) + \Phi_2 K_0(q_1 r)}{\Psi_1\Phi_1 + \Psi_2\Phi_2}\right] \tag{9}$$

and

$$\overline{H}_2 = \frac{r_w S_2 H_0}{q_1 r_s}\left[\frac{K_0(q_2 r)}{\Psi_1\Phi_1 + \Psi_2\Phi_2}\right] \tag{10}$$

where $q_1^2 = pS_1/T_1$; $q_2^2 = pS_2/T_2$; $\eta = S_2/S_1$; $\alpha = S_2 r_w^2/r_c^2$; p is the Laplace variable [28]; $I_0(\cdot)$ and $K_0(\cdot)$ are respectively the modified Bessel functions of the first and second kinds of order zero; and $I_1(\cdot)$ and $K_1(\cdot)$ are respectively the modified Bessel functions of the first and second kinds of order one. Variables Ψ_1, Ψ_2, Φ_1, and Φ_2 are respectively defined as

$$\Psi_1 = -\eta q_1 r_w I_0(q_1 r_w) + 2\alpha I_1(q_1 r_w) \tag{11}$$

$$\Psi_2 = \eta q_1 r_w K_0(q_1 r_w) + 2\alpha K_1(q_1 r_w) \tag{12}$$

$$\Phi_1 = T_1 q_1\left[-K_1(q_1 r_s)K_0(q_2 r_s) + \sqrt{\frac{S_2T_2}{S_1T_1}}K_0(q_1 r_s)K_1(q_2 r_s)\right] \tag{13}$$

and

$$\Phi_2 = T_1 q_1\left[I_1(q_1 r_s)K_0(q_2 r_s) + \sqrt{\frac{S_2T_2}{S_1T_1}}I_0(q_1 r_s)K_1(q_2 r_s)\right] \tag{14}$$

When $r = r_w$, the well water level in the Laplace domain, $\overline{H}_w$, obtained from Eq. (9) is

$$\overline{H}_w = \frac{r_w S_2 H_0}{T_1 q_1}\left[\frac{-\Phi_1 I_0(q_1 r_w) + \Phi_2 K_0(q_1 r_w)}{\Psi_1\Phi_1 + \Psi_2\Phi_2}\right] \tag{15}$$

The time-domain solutions of Eqs. (9) and (10) obtained using the Bromwich integral [13, p. 624] are respectively

$$H_1(r,t) = \frac{2\eta r_w H_0}{\pi}\int_0^\infty e^{-\frac{T_1}{S_1}u^2 t} \times \frac{A_1(r,u)B_1(u) + A_2(r,u)B_2(u)}{B_1^2(u) + B_2^2(u)}\,du \tag{16}$$

and

$$H_2(r,t) = \frac{4\eta r_w H_0}{\pi^2 r_s}\int_0^\infty e^{-\frac{T_1}{S_1}u^2 t} \times \frac{J_0(r\kappa u)B_2(u) - Y_0(r\kappa u)B_1(u)}{B_1^2(u) + B_2^2(u)}\,\frac{du}{u} \tag{17}$$

with

$$A_1(r,u) = [Y_1(r_s u)Y_0(r_s\kappa u)J_0(ru) - J_1(r_s u)Y_0(r_s\kappa u)Y_0(ru)] - \sqrt{\frac{S_2T_2}{S_1T_1}}[Y_0(r_s u)Y_1(r_s\kappa u)J_0(ru) - J_0(r_s u)Y_1(r_s\kappa u)Y_0(ru)] \tag{18}$$

$$A_2(r,u) = [J_1(r_s u)J_0(r_s\kappa u)Y_0(ru) - Y_1(r_s u)J_0(r_s\kappa u)J_0(ru)] - \sqrt{\frac{S_2T_2}{S_1T_1}}[J_0(r_s u)J_1(r_s\kappa u)Y_0(ru) - Y_0(r_s u)J_1(r_s\kappa u)J_0(ru)] \tag{19}$$

$$B_1(u) = \eta(r_w u)\left\{\begin{array}{l}[J_1(r_s u)J_0(r_s\kappa u)Y_0(r_w u) - Y_1(r_s u)J_0(r_s\kappa u)J_0(r_w u)] \\ \quad -\sqrt{\frac{S_2T_2}{S_1T_1}}[J_0(r_s u)J_1(r_s\kappa u)Y_0(r_w u) - Y_0(r_s u)J_1(r_s\kappa u)J_0(r_w u)]\end{array}\right\} - 2\alpha\left\{\begin{array}{l}[J_1(r_s u)J_0(r_s\kappa u)Y_1(r_w u) - Y_1(r_s u)J_0(r_s\kappa u)J_1(r_w u)] \\ \quad -\sqrt{\frac{S_2T_2}{S_1T_1}}[J_0(r_s u)J_1(r_s\kappa u)Y_1(r_w u) - Y_0(r_s u)J_1(r_s\kappa u)J_1(r_w u)]\end{array}\right\} \tag{20}$$

and

$$B_2(u) = \eta(r_w u)\left\{\begin{array}{l}[J_1(r_s u)Y_0(r_s\kappa u)Y_0(r_w u) - Y_1(r_s u)Y_0(r_s\kappa u)J_0(r_w u)] \\ \quad -\sqrt{\frac{S_2T_2}{S_1T_1}}[J_0(r_s u)Y_1(r_s\kappa u)Y_0(r_w u) - Y_0(r_s u)Y_1(r_s\kappa u)J_0(r_w u)]\end{array}\right\} - 2\alpha\left\{\begin{array}{l}[J_1(r_s u)Y_0(r_s\kappa u)Y_1(r_w u) - Y_1(r_s u)Y_0(r_s\kappa u)J_1(r_w u)] \\ \quad -\sqrt{\frac{S_2T_2}{S_1T_1}}[J_0(r_s u)Y_1(r_s\kappa u)Y_1(r_w u) - Y_0(r_s u)Y_1(r_s\kappa u)J_1(r_w u)]\end{array}\right\} \tag{21}$$

where u is a dummy variable and $\kappa = \sqrt{T_1 S_2 / T_2 S_1}$. Note that $J_0(\cdot)$ and $Y_0(\cdot)$ are respectively the Bessel functions of the first and second kinds of order zero; and $J_1(\cdot)$ and $Y_1(\cdot)$ are respectively the Bessel functions of the first and second kinds of order one. Eqs. (16) and (17) are the closed-form solutions for hydraulic head distributions in the skin and formation zones, respectively. The detailed derivation of Eq. (16) is described in Appendix A. Eq. (17) for hydraulic head distribution in the formation can be obtained in a similar manner.

From Eq. (16), the change of water level in the well, i.e., $r = r_w$, is

$$H_w(r_w, t) = \frac{2\eta r_w H_0}{\pi} \int_0^\infty e^{-\frac{T_1}{S_1}u^2 t} \times \frac{A_{1w}(u)B_1(u) + A_{2w}(u)B_2(u)}{B_1^2(u) + B_2^2(u)}\, du \tag{22}$$

with

$$A_{1w}(r_w, u) = [Y_1(r_s u)Y_0(r_s \kappa u)J_0(r_w u) - J_1(r_s u)Y_0(r_s \kappa u)Y_0(r_w u)] - \sqrt{\frac{S_2 T_2}{S_1 T_1}}[Y_0(r_s u)Y_1(r_s \kappa u)J_0(r_w u) - J_0(r_s u)Y_1(r_s \kappa u)Y_0(r_w u)] \tag{23}$$

and

$$A_{2w}(r_w, u) = [J_1(r_s u)J_0(r_s \kappa u)Y_0(r_w u) - Y_1(r_s u)J_0(r_s \kappa u)J_0(r_w u)] - \sqrt{\frac{S_2 T_2}{S_1 T_1}}[J_0(r_s u)J_1(r_s \kappa u)Y_0(r_w u) - Y_0(r_s u)J_1(r_s \kappa u)J_0(r_w u)] \tag{24}$$

2.3. Dimensionless solutions

The dimensionless hydraulic head, h, is usually defined as

$$h = \frac{H_0 - H(t)}{H_0 - H_i} \tag{25}$$

where H_i is the well water level immediately after removal or injection and $H(t)$ is the well water level at time t.

Dimensionless parameters are defined as

$$\beta = \frac{T_2 t}{r_c^2}, \quad \zeta = \frac{T_2}{T_1}, \quad \rho = \frac{r}{r_w}, \quad \rho_c = \frac{r_c}{r_w}, \quad \rho_s = \frac{r_s}{r_w} \tag{26}$$

where β is dimensionless time; ζ is a ratio of formation transmissivity to skin transmissivity; ρ is the dimensionless distance from the centerline of well; ρ_c is the dimensionless radius of standpipe; and ρ_s is the dimensionless radial distance from the centerline of well to the outer skin envelope. The positive skin is defined for $\zeta > 1$ and the negative skin for $\zeta < 1$. Also, an aquifer is homogeneous and no skin exists when $\zeta = 1$ and may be called a uniform aquifer.

The Laplace-domain solutions, Eqs. (9), (10), and (15), can respectively be expressed in dimensionless form as

$$\bar{h}_1 = \zeta\left[\frac{-\phi_1 I_0(\lambda_1\rho) + \phi_2 K_0(\lambda_1\rho)}{\psi_1\phi_1 + \psi_2\phi_2}\right] \tag{27}$$

$$\bar{h}_2 = \frac{\zeta}{\rho_s}\left[\frac{K_0(\lambda_2\rho)}{\psi_1\phi_1 + \psi_2\phi_2}\right] \tag{28}$$

and

$$\bar{h}_w = \zeta\left[\frac{-\phi_1 I_0(\lambda_1) + \phi_2 K_0(\lambda_1)}{\psi_1\phi_1 + \psi_2\phi_2}\right] \tag{29}$$

where $\lambda_1^2 = \zeta p/\eta$; $\lambda_2^2 = p$; and

$$\psi_1 = -\zeta p I_0(\lambda_1) + 2\alpha\lambda_1 I_1(\lambda_1) \tag{30}$$

$$\psi_2 = \zeta p K_0(\lambda_1) + 2\alpha\lambda_1 K_1(\lambda_1) \tag{31}$$

$$\phi_1 = -\lambda_1 K_1(\lambda_1\rho_s)K_0(\lambda_2\rho_s) + \zeta\lambda_2 K_0(\lambda_1\rho_s)K_1(\lambda_2\rho_s) \tag{32}$$

and

$$\phi_2 = \lambda_1 I_1(\lambda_1\rho_s)K_0(\lambda_2\rho_s) + \zeta\lambda_2 I_0(\lambda_1\rho_s)K_1(\lambda_2\rho_s) \tag{33}$$

Note that the Laplace-domain solutions of Eqs. (27)–(29) were also given in Moench and Hsieh [22].

Similarly, the time-domain solutions for head distributions in the skin and formation zones, Eqs. (16) and (17), can be respectively expressed in dimensionless form as

$$h_1(\rho, \beta) = \frac{2\eta}{\pi} \int_0^\infty e^{-\frac{\eta\beta}{\zeta\alpha}\tau w^2} \times \frac{A_1(\rho, w)B_1(w) + A_2(\rho, w)B_2(w)}{B_1^2(w) + B_2^2(w)}\, dw \tag{34}$$

and

$$h_2(\rho, \beta) = \frac{2\eta}{\pi} \int_0^\infty e^{-\frac{\eta\beta}{\zeta\alpha}\tau w^2} \frac{2}{\pi\rho_s} \times \frac{J_0(\rho\kappa w)B_2(w) - Y_0(\rho\kappa w)B_1(w)}{B_1^2(w) + B_2^2(w)} \frac{dw}{w} \tag{35}$$

where $w = r_w u$; and

$$A_1(\rho, w) = [Y_1(\rho_s w)Y_0(\rho_s \kappa w)J_0(\rho w) - J_1(\rho_s u)Y_0(\rho_s \kappa w)Y_0(\rho w)] - \sqrt{\zeta\eta}[Y_0(\rho_s w)Y_1(\rho_s \kappa w)J_0(\rho w) - J_0(\rho_s w)Y_1(\rho_s \kappa w)Y_0(\rho w)] \quad (36)$$

$$A_2(\rho, w) = [J_1(\rho_s w)J_0(\rho_s \kappa w)Y_0(\rho w) - Y_1(\rho_s w)J_0(\rho_s \kappa w)J_0(\rho w)] - \sqrt{\zeta\eta}[J_0(\rho_s w)J_1(\rho_s \kappa w)Y_0(\rho w) - Y_0(\rho_s w)J_1(\rho_s \kappa w)J_0(\rho w)] \quad (37)$$

$$B_1(w) = (\eta w)\left\{ \begin{array}{l} [J_1(\rho_s w)J_0(\rho_s \kappa w)Y_0(w) - Y_1(\rho_s w)J_0(\rho_s \kappa w)J_0(w)] \\ \quad -\sqrt{\zeta\eta}[J_0(\rho_s w)J_1(\rho_s \kappa w)Y_0(w) - Y_0(\rho_s w)J_1(\rho_s \kappa w)J_0(w)] \end{array} \right\} - 2\alpha\left\{ \begin{array}{l} [J_1(\rho_s w)J_0(\rho_s \kappa u)Y_1(w) - Y_1(\rho_s w)J_0(\rho_s \kappa u)J_1(w)] \\ \quad -\sqrt{\zeta\eta}[J_0(\rho_s w)J_1(\rho_s \kappa w)Y_1(w) - Y_0(\rho_s w)J_1(\rho_s \kappa w)J_1(w)] \end{array} \right\} \quad (38)$$

and

$$B_2(w) = (\eta w)\{ [J_1(\rho_s w)Y_0(\rho_s \kappa w)Y_0(w) - Y_1(\rho_s w)Y_0(\rho_s \kappa w)J_0(w)] - \sqrt{\zeta\eta}[J_0(\rho_s w)Y_1(\rho_s \kappa w)Y_0(w) - Y_0(\rho_s w)Y_1(\rho_s \kappa w)J_0(w)] \} - 2\alpha\{ [J_1(\rho_s w)Y_0(\rho_s \kappa w)Y_1(w) - Y_1(\rho_s w)Y_0(\rho_s \kappa w)J_1(w)] - \sqrt{\zeta\eta}[J_0(\rho_s w)Y_1(\rho_s \kappa w)Y_1(w) - Y_0(\rho_s w)Y_1(\rho_s \kappa w)J_1(w)] \} \quad (39)$$

In addition, the dimensionless water level at a well, Eq. (22), can also be expressed as

$$h_w(1, \beta) = \frac{2\eta}{\pi}\int_0^\infty e^{-\frac{\eta\beta}{\zeta\alpha}w^2} \times \frac{A_{1w}(w)B_1(w) + A_{2w}(w)B_2(w)}{B_1^2(w) + B_2^2(w)}\, dw \quad (40)$$

where

$$A_{1w}(1, w) = [Y_1(\rho_s w)Y_0(\rho_s \kappa w)J_0(w) - J_1(\rho_s u)Y_0(\rho_s \kappa w)Y_0(w)] - \sqrt{\zeta\eta}[Y_0(\rho_s w)Y_1(\rho_s \kappa w)J_0(w) - J_0(\rho_s w)Y_1(\rho_s \kappa w)Y_0(w)] \quad (41)$$

and

$$A_{2w}(1, w) = [J_1(\rho_s w)J_0(\rho_s \kappa w)Y_0(w) - Y_1(\rho_s w)J_0(\rho_s \kappa w)J_0(w)] - \sqrt{\zeta\eta}[J_0(\rho_s w)J_1(\rho_s \kappa w)Y_0(w) - Y_0(\rho_s w)J_1(\rho_s \kappa w)J_0(w)] \quad (42)$$

3. Verification of solutions

The Laplace-domain solutions, Eqs. (9) and (10), and the time-domain solutions, Eqs. (34) and (35), for a two-zone aquifer system are compared with the existing solution for a uniform aquifer under the same well configuration and geologic formation. The Laplace-domain solution for the hydraulic head in a uniform medium presented by Cooper et al. [8] is

$$\overline{H} = \frac{H_0 r_w S K_0(qr)}{Tq[qr_w K_0(qr_w) + 2\alpha K_1(qr_w)]} \quad (43)$$

It can be shown that both Eqs. (9) and (10) reduce to Eq. (43) if the hydraulic properties of the skin are equal to the hydraulic properties of the aquifer, i.e., $\zeta = \eta = 1$. Similarly, Eqs. (34) and (35) reduce to

$$h(\rho, \beta) = \frac{2}{\pi}\int_0^\infty e^{-\frac{\beta}{\alpha}w^2} \times \frac{J_0(\rho w)[wY_0(w) - 2\alpha Y_1(w)] - Y_0(\rho w)[wJ_0(w) - 2\alpha J_1(w)]}{[wJ_0(w) - 2\alpha J_1(w)]^2 + [wY_0(w) - 2\alpha Y_1(w)]^2}\, dw \quad (44)$$

which indeed is the solution presented by Cooper et al. [8] for dimensionless hydraulic head distribution in a uniform medium.

The Laplace-domain solution of Eq. (29) and the time-domain solution of Eq. (40) for a well water level consist of products of Bessel functions. These functions are approximated by the formulas given in Abramowitz and Stegun [1] and Watson [29] and the function evaluations are accelerated using the Shanks method [27,30,32]. The values of Bessel functions in Eqs. (29) and (40) are computed at least to ten decimal places, and thus have the same accuracy as those listed in Abramowitz and Stegun [1]. The work valuated the Bessel functions has been presented in Yang and Yeh [32]. The inverse Laplace transform of Eq. (29) is evaluated by the routine INLAP of IMSL [14] with accuracy to five decimal places. This routine was developed based on an algorithm originally proposed by Crump [9] and modified by de Hoog et al. [10]. This method approximates the Laplace inversion by expressing the transformed function in a Fourier series.

Fig. 2 illustrates the curves of the integrand in Eq. (40) versus w for $\rho_c = 0.5$, $\rho_s = 10$, $\eta = 1$, $\beta = 0.1$, and

$\alpha = 10^{-1}$ when $\zeta = 0.1$, 1 or 10. The figure shows that these curves oscillate over some cycles and quickly die out if the skin presents ($\zeta \neq 1$). On the other hand, the curve only has a single peak for a uniform medium ($\zeta = 1$). Thus, the closed-form solution for dimensionless water level at the well, Eq. (40), can be easily evaluated by using a numerical integration approach. The integration is carried out by the Gaussian quadrature for the ranges from zero to infinite. The approach of numerical calculations for Eq. (40) is similar to that of Yeh et al. [33].

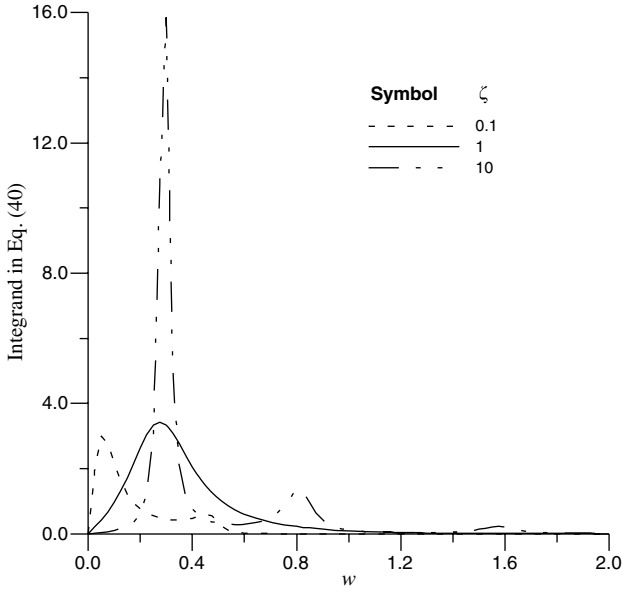

Fig. 2. A plot of the integrand in Eq. (40) versus w for $\rho_c = 0.5$, $\rho_s = 10$, $\eta = 1$, $\beta = 0.1$, and $\alpha = 0.1$ when $\zeta = 0.1$, 1 or 10.

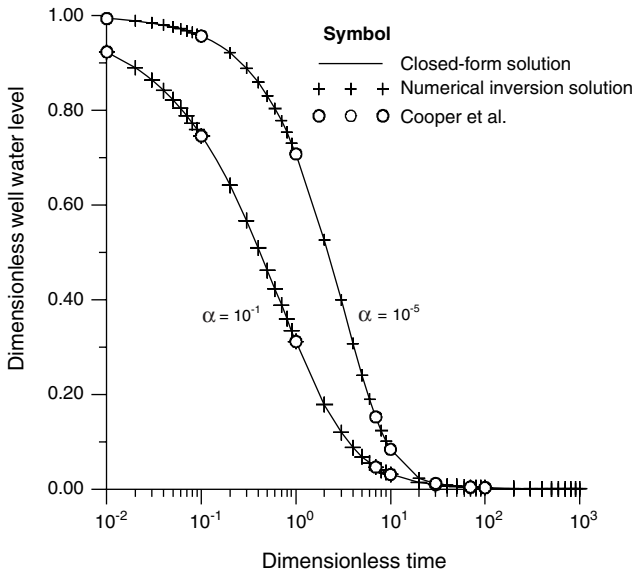

Fig. 3. Plots of dimensionless well water level versus dimensionless time (β) estimated by the closed-form solution, the numerical inversion from the Laplace-domain solution, and those given in Cooper et al. [8] for $\rho_c = 0.5$, $\rho_s = 10$, and $\zeta = \eta = 1$ when $\alpha = 10^{-1}$ or 10^{-5}.

Comparisons between the evaluated results of the closed-form solution of Eq. (40) and those obtained by a numerical inversion from Eq. (29) provide a cross check for the accuracy of both solutions. Under a uniform medium condition ($\zeta = \eta = 1$), Fig. 3 shows the

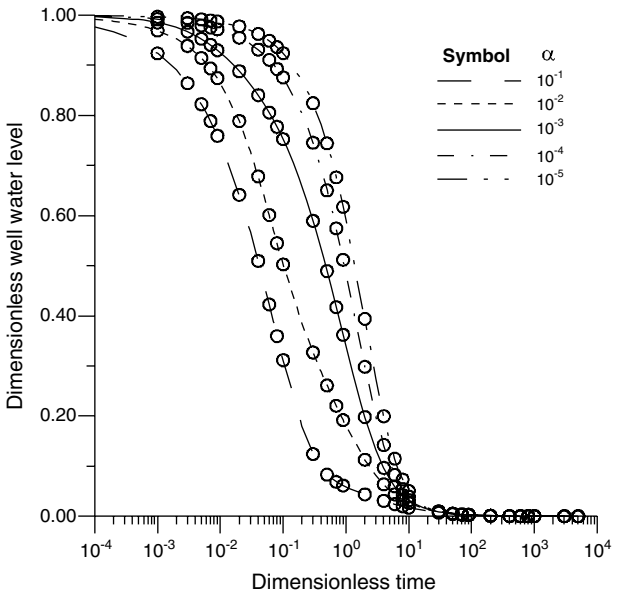

Fig. 4. Plots of dimensionless well water level versus dimensionless time (β) estimated by the closed-form solution and the numerical inversion from the Laplace-domain solution for $\rho_c = 0.5$, $\rho_s = 10$, $\eta = 1$, and $\alpha = 10^{-1}$–10^{-5} when $\zeta = 0.1$. The line presents the closed-form solution and the circle presents the numerical inversion from the Laplace-domain solution.

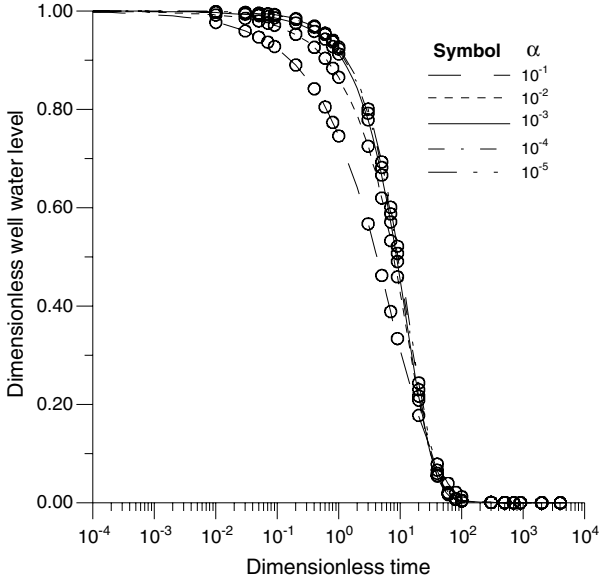

Fig. 5. Plots of dimensionless well water level versus dimensionless time (β) estimated by the closed-form solution and the numerical inversion from the Laplace-domain solution for $\rho_c = 0.5$, $\rho_s = 10$, $\eta = 1$, and $\alpha = 10^{-1}$–10^{-5} when $\zeta = 10$. The line presents the closed-form solution and the circle presents the numerical inversion from the Laplace-domain solution.

curves of dimensionless well water level versus dimensionless time (β) for $\rho_c = 0.5$ and $\rho_s = 10$ when $\alpha = 10^{-1}$ or 10^{-5}. The figure indicates that the results obtained by a numerical Laplace inversion agree extremely well with those of the closed-form solution and Cooper et al. [8]. Under a two-zone condition, the dimensionless well water level versus dimensionless time with $\rho_c = 0.5$, $\rho_s = 10$, $\eta = 1$, and $\alpha = 10^{-1}$–10^{-5} are shown in Fig. 4 for $\zeta = 0.1$ and in Fig. 5 for $\zeta = 10$. The values of dimensionless well water level obtained by a numerical Laplace inversion are consistent with those of the closed-form solution to five decimal places. This indicates that the closed-form solution for a two-zone system yields correctly evaluated results when estimated by a numerical approach. Note that the modified Crump method fails to converge for the Laplace-domain solution when the dimensionless time is very small ($\beta < 0.001$ for $\zeta = 0.1$ and $\beta < 0.01$ for $\zeta = 10$) as indicated in Figs. 4 and 5. In contrast, the numerical integration approach applied to the time-domain solution works well for all range of dimensionless times.

4. Results and discussion

The curves of dimensionless well water level versus dimensionless time are developed to investigate the impacts of the skin type, skin thickness, and the contrast of skin transmissivity to formation transmissivity on dimensionless head distribution. For ease of comparisons, η and ρ_c are respectively chosen as one and 0.5. In addition, all function evaluations for these solutions

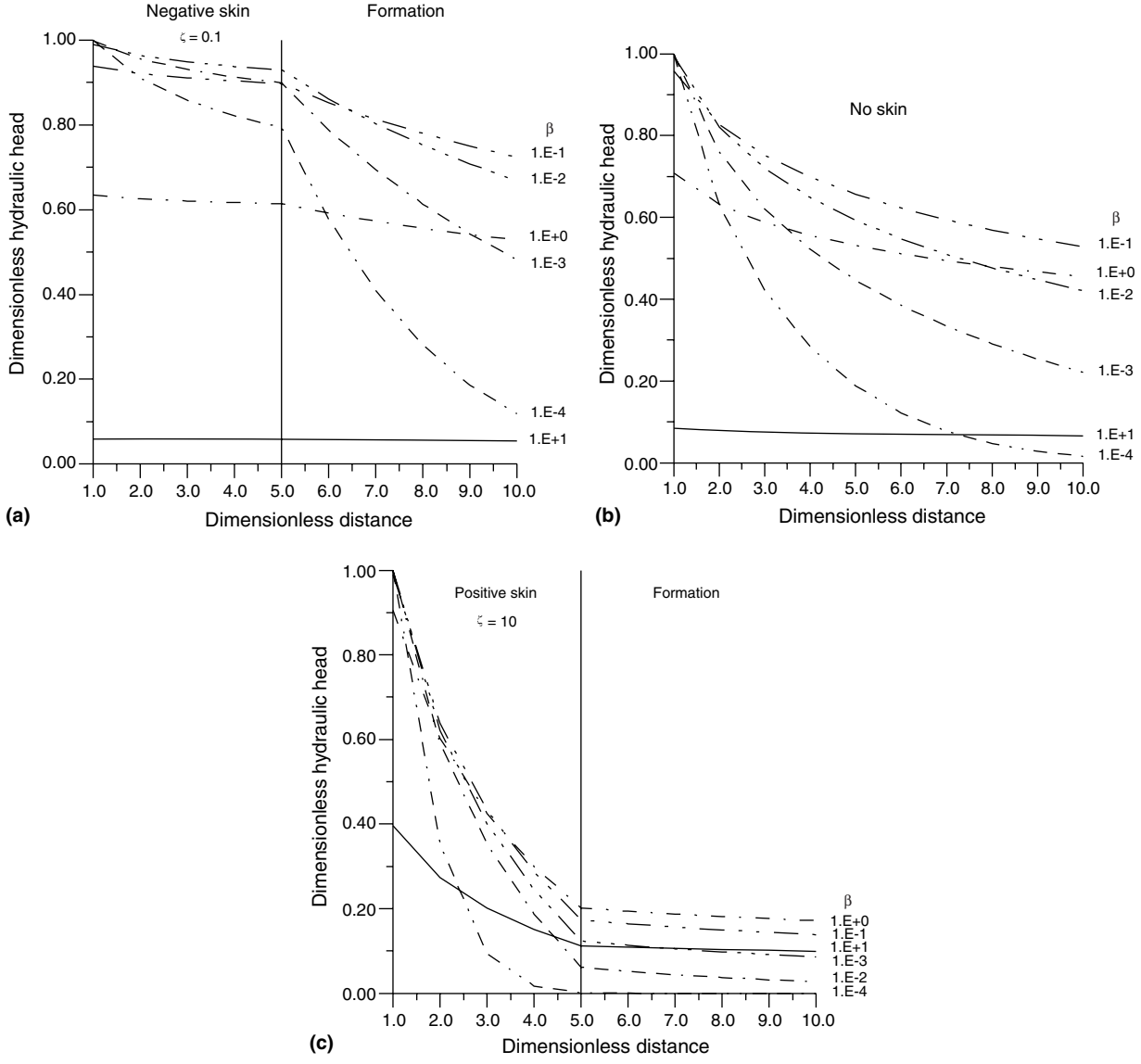

Fig. 6. Plots of dimensionless hydraulic head versus dimensionless time for $\rho_s = 5$, $\alpha = 10^{-5}$, and $\beta = 10^{-4}$ to 10 when (a) $\zeta = 0.1$, (b) $\zeta = 1$, and (c) $\zeta = 10$.

are under double precision and accurate to five decimal places.

4.1. Effect of skin type

Fig. 6 displays the curves of dimensionless hydraulic head versus dimensionless distance for $\rho_s = 5$, $\alpha = 10^{-5}$, and β ranging from 10^{-4} to 10 when (a) $\zeta = 0.1$, (b) $\zeta = 1$, and (c) $\zeta = 10$. For the case without a skin zone, the dimensionless hydraulic head gradually decreases when increasing radial distance as shown in Fig. 6b. If a finite-thickness skin the present, both Fig. 6a and c demonstrate that the relation of dimensionless hydraulic head versus dimensionless distance exhibits two curves with different slope joined at the interface ($\rho_s = 5$). A negative skin, which has a higher transmissivity than the formation, has a curve with relative mild slope in the skin zone and with steeper slope in the formation zone. In contrast, a positive skin has a very steep slope in the skin zone due to the lower transmissivity and a relative flat slope in the formation zone. The dimensionless hydraulic head at the well always decreases with increasing dimensionless time (β); on the other hand, the dimensionless hydraulic head in the formation zone increases at the beginning of the test, and then decreases at large-dimensionless time (say, $\beta > 1$ or 10). In addition, the dimensionless hydraulic head for an aquifer with a negative skin stabilizes more quickly than that with a positive skin.

4.2. Effect of skin thickness

Fig. 7 displays two sets of curves to investigate the influence of skin thickness ($r_s - r_w$) on dimensionless well water level for $\alpha = 10^{-5}$ and $\rho_s = 5$, 10, 50, and 100 when $\zeta = 0.1$ or 10. The figure indicates that the dimensionless skin thickness (i.e., $\rho_s - 1$) effects the dimensionless well water level at intermediate time, as β ranging from 0.01 to 10 for $\zeta = 0.1$ and from 1 to 100 for $\zeta = 10$. However, the dimensionless well water level diminishes to zero at large-dimensionless time. For a positive skin condition, the dimensionless well water level increases with dimensionless skin thickness. A larger dimensionless well water level reflects the effect of a smaller hydraulic conductivity for a positive skin. In contrast, the dimensionless well water level decreases as dimensionless skin thickness increases if a negative skin is present.

4.3. Effect of contrast of skin transmissivity to formation transmissivity

A plot of dimensionless well water level versus dimensionless time for $\rho_s = 10$ and $\alpha = 10^{-5}$ when $\zeta = 0.1$, 0.5, 1, 5, and 10 is displayed in Fig. 8. This figure shows the curves of dimensionless well water level for the system under the conditions with no skin (i.e., $\zeta = 1$), negative skin (i.e., $\zeta = 0.1$ or 0.5), and positive skin (i.e., $\zeta = 5$ or 10). A smaller transmissivity of a positive skin (in contrast to aquifer transmissivity) produces a smaller flow rate from the well toward the formation and results in a higher dimensionless well water level. Therefore, a larger value of ζ has a higher dimensionless well water level. On the other hand, a larger transmissivity of a negative skin (in contrast to aquifer transmissivity) yields a larger flow rate across the wellbore and results in a lower dimensionless well water level. Thus, a smaller value of ζ results in a lower dimensionless well water level. The

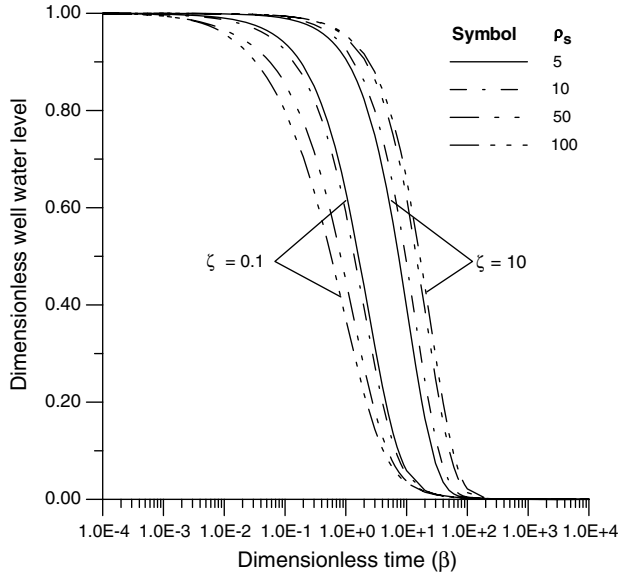

Fig. 7. A plot of dimensionless well water level versus dimensionless time for $\alpha = 10^{-5}$ and $\rho_s = 5$, 10, 50, and 100 when $\zeta = 0.1$ or 10.

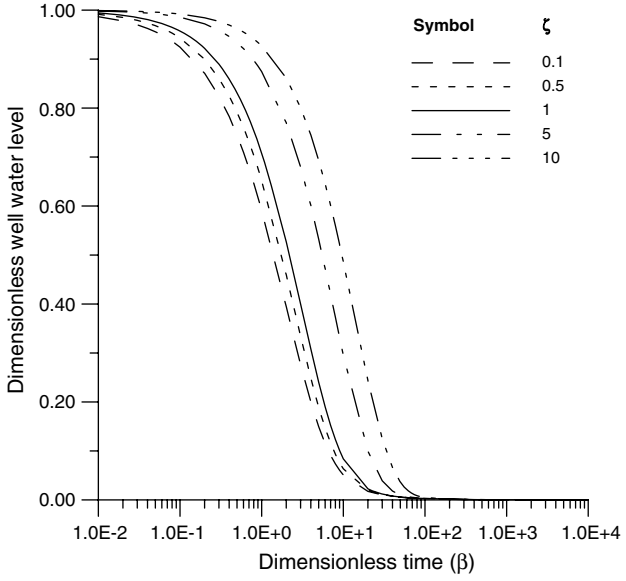

Fig. 8. A plot of dimensionless well water level versus dimensionless time for $\rho_s = 10$ and $\alpha = 10^{-5}$ when $\zeta = 0.1$, 0.5, 1, 5, and 10.

figure demonstrates that the system with a positive skin has the highest dimensionless well water levels, the system without the skin give the second highest, and the one with a negative skin yield the lowest at the same dimensionless time. Fig. 8 also indicates that the differences of dimensionless well water level between the two-zone and uniform medium systems are negligibly small at small- and large-dimensionless times (say, $\beta < 10^{-1}$ and $\beta > 10^{2}$). Contrarily, the differences of dimensionless well water level for the system under different skin condition are quite large at intermediate-dimensionless time.

5. Conclusions

A new analytical solution (in the time domain) has been developed for slug tests in a well, which is installed in a radial confined aquifer system with a finite-thickness skin. This solution is derived from a radial two-zone ground-water flow equation using Laplace transforms and the Bromwich integral. In a uniform medium condition, the dimensionless well water levels computed from the closed-form solution agree very well with these of the Laplace-domain solution and Cooper et al. [8]. We have shown that numerical inversion fails to evaluate the Laplace-domain solution if the dimensionless time is very small. On the other hand, the present analytical solution can be evaluated numerically for the entire time domain with accuracy to the fifth decimal place.

Under a radial two-zone condition, i.e., with a positive or negative skin, the dimensionless well water levels computed from the closed-form solution match with those of the Laplace-domain solution to at least five decimal places. This provides a double check to make sure that the closed-form and Laplace-domain solutions are correctly evaluated. The distributions of dimensionless hydraulic head in a uniform medium are significantly different from these in a two-zone aquifer with a positive or negative skin. The relation of dimensionless hydraulic head versus dimensionless distance exhibits two curves with different slope joined at the interface. The dimensionless hydraulic head of a negative skin more quickly stabilizes than that of a positive skin. Obviously, the magnitude of dimensionless hydraulic head strongly depends on the hydraulic properties of both the skin and formation zones.

The dimensionless skin thickness affects the dimensionless well water level at intermediate-dimensionless time. The dimensionless well water level increases with dimensionless positive skin thickness and decreases as dimensionless negative skin thickness increases. The distributions of dimensionless well water level in a two-zone aquifer system significantly differ from those in a uniform medium. The dimensionless well water levels are smaller for the system with a negative skin than those with a positive skin at the same dimensionless time. The difference of dimensionless well water level between the two-zone and uniform medium systems decreases significantly with α because a smaller storage coefficient has less effect on dimensionless well water level.

Acknowledgements

This study was partly supported by the Taiwan National Science Council under the Grant NSC 92-2211-E-009-008. The authors appreciate the comments and suggested revisions of three anonymous reviewers that help improve the clarity of our presentation.

Appendix A. Derivation of Eq. (16)

The inverse Laplace transforms of Eq. (9) in the time domain can be obtained using the Bromwich integral [13] as

$$H_1 = \frac{1}{2\pi \mathrm{i}} \int_{\xi-\mathrm{i}\infty}^{\xi+\mathrm{i}\infty} \mathrm{e}^{pt} \overline{H}_1 \, \mathrm{d}p \tag{A.1}$$

where p = complex variable, i = imaginary unit, and ξ = large, real, and positive constant, so that all the poles lie to the left of line $(\xi - \mathrm{i}\infty, \xi + \mathrm{i}\infty)$.

A single branch point with no singularity (pole) at $p = 0$ exists in the integrand of Eq. (9). Thus, this integral requires the Bromwich integral for the Laplace inversion. The closed contour of integrand is shown in

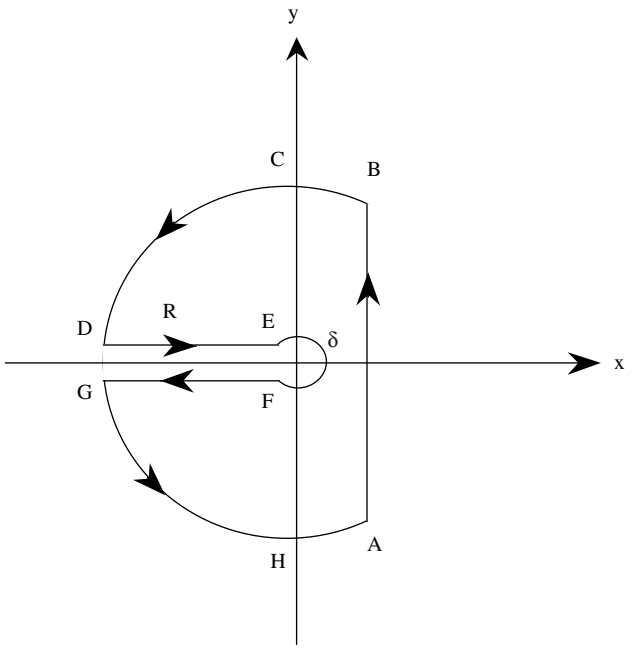

Fig. 9. A plot of the closed contour integration of $\overline{H}$ for the Bromwich integral [13].

Fig. 9 with a cut of p plane along a negative real axis, where δ is taken sufficiently small to exclude all poles from the circle about the origin. The closed contour consists of the part AB of the Bromwich line from minus infinity to infinity, semicircles BCD and GHA of radius R, lines DE and FG parallel to the real axis, and a circle EF of radius δ about a origin. The integration along the small circle EF around an origin as δ approaches zero is carried out using the Cauchy integral and the value of the integral is equal to zero. The integrals taken along BCD and GHA tend to zero as R approaches infinity. Consequently, Eq. (9) can be replaced by the sum of integrals along DE and FG. In other words, the integral can be written as

$$H_1 = \lim_{\substack{\delta\to 0\\ R\to\infty}} \frac{1}{2\pi \mathrm{i}}\left[\int_{DE} \mathrm{e}^{pt}\overline{H}_1\,\mathrm{d}p + \int_{FG} \mathrm{e}^{pt}\overline{H}_1\,\mathrm{d}p\right] \tag{A.2}$$

For the first term on the right-hand-side (RHS) of Eq. (A.2) along DE, we introduce the new variable $p = u^2\mathrm{e}^{-\pi \mathrm{i}}T_1/S_1$ and use the formulas [6, p. 490]

$$K_v\left(z\mathrm{e}^{\pm\frac{1}{2}\pi \mathrm{i}}\right) = \pm\frac{1}{2}\pi \mathrm{i}\mathrm{e}^{\mp\frac{1}{2}v\pi \mathrm{i}}[-J_v(z) \pm \mathrm{i}Y_v(z)] \tag{A.3}$$

and

$$I_v\left(z\mathrm{e}^{\pm\frac{1}{2}\pi \mathrm{i}}\right) = \mathrm{e}^{\pm\frac{1}{2}v\pi \mathrm{i}}J_v(z) \tag{A.4}$$

where $v = 0, 1, 2, \ldots$The first term on the RHS of Eq. (A.2) then leads to

$$H_{1DE} = -\frac{r_\mathrm{w}\eta H_0}{\pi \mathrm{i}}\int_0^\infty \mathrm{e}^{-\frac{T_1}{S_1}u^2 t}\frac{[A_2(u) - \mathrm{i}A_1(u)]}{[B_1(u) + \mathrm{i}B_2(u)]}\,\mathrm{d}u \tag{A.5}$$

Likewise, introducing $p = u^2\mathrm{e}^{\pi \mathrm{i}}T_1/S_1$, the integral along FG gives minus the conjugate of Eq. (A.5) as

$$H_{1FG} = \frac{r_\mathrm{w}\eta H_0}{\pi \mathrm{i}}\int_0^\infty \mathrm{e}^{-\frac{T_1}{S_1}u^2 t}\frac{[A_1(u) + \mathrm{i}A_2(u)]}{[B_1(u) - \mathrm{i}B_2(u)]}\,\mathrm{d}u \tag{A.6}$$

The closed-form solution of Eq. (16) can then be obtained by combining Eqs. (A.5) and (A.6).

References

[1] Abramowitz M, Stegun IA. Handbook of mathematical functions with formulas, graphs and mathematical tables. National Bureau of Standards. Washington: Dover; 1964.

[2] Bouwer H. The Bouwer and Rice slug test—an update. Ground Water 1989;27(3):304–9.

[3] Bouwer H, Rice RC. A slug test for determining hydraulic conductivity of unconfined aquifers with completely or partially penetrating wells. Water Res Res 1976;12(3):423–8.

[4] Bredehoeft JD, Cooper Jr HH, Papadopulos IS. Inertial and storage effects in well-aquifer systems: an analog investigation. Water Res Res 1966;2(4):697–707.

[5] Butler Jr JJ, Healey JM. Relationship between pumping-test and slug-test parameters: scale effect or artifact? Ground Water 1998;36(2):305–13.

[6] Carslaw HS, Jaeger JC. Conduction of heat in solids. 2nd ed. Oxford: Clarendon; 1959.

[7] Charbeneau RJ. Groundwater hydraulic and pollutant transport. Upper Saddle River, NJ: Prentice-Hall; 2000.

[8] Cooper Jr HH, Bredehoeft JD, Papadopulos IS. Response of a finite-diameter well to an instantaneous charge of water. Water Res Res 1967;3(1):263–9.

[9] Crump KS. Numerical inversion of Laplace transforms using a Fourier series approximation. J Assoc Comput Mach 1976;23(1):89–96.

[10] de Hoog FR, Knight JH, Stokes AN. An improved method for numerical inversion of Laplace transforms. Society for Industrial and Applied Mathematics. J Sci Stat Comput 1982;3(3):357–66.

[11] Faust CR, Mercer JW. Evaluation of slug tests in wells containing a finite-thickness skin. Water Res Res 1984;20(4):504–6.

[12] Ferris JG, Knowles DB. The slug test for estimating transmissibility. US Geol Survey Ground Water 1954;26:1–7.

[13] Hildebrand FB. Advanced calculus for applications. 2nd ed. Englewood Cliffs, New Jersey: Prentice-Hall; 1976.

[14] IMSL. MATH/Library. vol. 1. Houston, TX: Visual Numerics; 1997.

[15] Karasaki K. A systematized drill-stem test. Water Res Res 1990;26(12):2913–9.

[16] Karasaki K, Long JCS, Witherspoon PA. Analytical models of slug tests. Water Res Res 1988;24(1):115–26.

[17] Kipp Jr KL. Type curve analysis of inertial effects in the response of a well to a slug test. Water Res Res 1985;21(9):1397–408.

[18] Kreyszig E. Advanced engineering mathematics. 7th ed. New York: John Wiley & Sons; 1993.

[19] Lohman SW. Ground-water hydraulics. US Geological Survey Professional Paper, vol. 708, 1972. p. 70.

[20] Marschall P, Barczewski B. The analysis of slug tests in the frequency domain. Water Res Res 1989;25(11):2388–96.

[21] Moench AF, Hsieh PA. Comment on "Evaluation of slug tests in wells containing a finite-thickness skin" by C. R. Faust and J.W. Mercer. Water Res Res 1985;21(9):1459–61.

[22] Moench AF, Hsieh PA. Analysis of slug test data in a well with finite thickness skin. In: The I.A.H. 17th International congress on hydrology of rocks of low permeability, International Association of Hydrogeol, Tucson, Ariz, January 1985. p. 7–12.

[23] Pandit NS, Miner RF. Interpretation of slug test data. Ground Water 1986;24(6):743–9.

[24] Ramey Jr HJ, Agarwal RG. Annulus unloading rates as influenced by wellbore storage and skin effect. Soc Petrol Eng J 1972:453–63.

[25] Ramey Jr HJ, Agarwal RG, Martin I. Analysis of "slug test" or DST flow period data. J Can Petrol Technol 1975:37–47.

[26] Sageev A. Slug test analysis. Water Res Res 1986;22(8):1323–33.

[27] Shanks D. Non-linear transformations of divergent and slowly convergent sequences. J Math Phys 1955;34:1–42.

[28] Spiegel MR. Laplace transforms. New York: Schaum; 1965.

[29] Watson GN. A treatise on the theory of Bessel functions. 2nd ed. Cambridge, UK: Cambridge University Press; 1958.

[30] Wynn P. On a device for computing the $e_m(S_n)$ transformation. Math Tables Other Aids Comput 1956;10:91–6.

[31] Yang YJ, Gates TM. Wellbore skin effect in slug-test data analysis for low-permeability geologic materials. Ground Water 1997;35(6):931–7.

[32] Yang SY, Yeh HD. A solution for flow rates across the wellbore in a two-layer confined aquifer. J Hydraul Eng ASCE 2002;128(2):175–83.

[33] Yeh HD, Yang SY, Peng HY. A new closed-form solution for radial two-layer draw down equation under constant-flux pumping in a finite-radius well. Adv Water Resour 2003;26(5):747–57.